MOLECULAR AND CELLULAR BIOLOGY, Oct. 2011, p. 4205–4218 Vol. 31, No. 20
0270-7306/11/$12.00 doi:10.1128/MCB.05893-11

Reducing Plasma Membrane Sphingomyelin Increases Insulin Sensitivity▽

Zhiqiang Li,[1]† Hongqi Zhang,[1,5]† Jing Liu,[1]† Chien-Ping Liang,[2] Yan Li,[1] Yue Li,[1] Gladys Teitelman,[1] Thomas Beyer,[3] Hai H. Bui,[3] David A. Peake,[3] Youyan Zhang,[3] Phillip E. Sanders,[3] Ming-Shang Kuo,[3] Tae-Sik Park,[4] Guoqing Cao,[3] and Xian-Cheng Jiang[1]*

Department of Cell Biology, State University of New York, Downstate Medical Center, Brooklyn, New York 11203[1]; Department of Medicine, Columbia University, New York, New York 10032[2]; Lilly Research Laboratories, Eli Lilly & Company, Indianapolis, Indiana 46285[3]; Department of Medicine, Lee Gil Ya Cancer and Diabetes Institute, Gachon University of Medicine and Science, Incheon, South Korea[4]; and Histology and Embryology, Shanghai Medical College, Fudan University, Shanghai, China[5]

Received 2 July 2011/Returned for modification 15 July 2011/Accepted 5 August 2011

It has been shown that inhibition of *de novo* sphingolipid synthesis increases insulin sensitivity. For further exploration of the mechanism involved, we utilized two models: heterozygous serine palmitoyltransferase (SPT) subunit 2 (*Sptlc2*) gene knockout mice and sphingomyelin synthase 2 (*Sms2*) gene knockout mice. SPT is the key enzyme in sphingolipid biosynthesis, and Sptlc2 is one of its subunits. Homozygous *Sptlc2*-deficient mice are embryonic lethal. However, heterozygous *Sptlc2*-deficient mice that were viable and without major developmental defects demonstrated decreased ceramide and sphingomyelin levels in the cell plasma membranes, as well as heightened sensitivity to insulin. Moreover, these mutant mice were protected from high-fat diet-induced obesity and insulin resistance. SMS is the last enzyme for sphingomyelin biosynthesis, and SMS2 is one of its isoforms. *Sms2* deficiency increased cell membrane ceramide but decreased SM levels. *Sms2* deficiency also increased insulin sensitivity and ameliorated high-fat diet-induced obesity. We have concluded that *Sptlc2* heterozygous deficiency- or *Sms2* deficiency-mediated reduction of SM in the plasma membranes leads to an improvement in tissue and whole-body insulin sensitivity.

Metabolic syndrome is a collection of abnormalities in metabolism, including obesity, nonalcoholic fatty liver disease, macrophage inflammation, impaired fasting glucose clearance, dyslipidemia, and hypertension. Insulin resistance appears to be a key feature in metabolic syndrome (47). The *de novo* sphingolipid synthesis pathway is considered a promising target for pharmacological intervention in insulin resistance. It has been shown that inhibition of serine palmitoyltransferase (SPT; the first enzyme for sphingolipid biosynthesis) increases insulin sensitivity (17). However, the mechanism is incompletely understood, since such an inhibition decreases many bioactive sphingolipids, including sphingomyelin (44), ceramide, and glycosphingolipids. Ceramide levels appear to be important in mediating inflammation, obesity, and insulin sensitivity (4, 17, 18). Sphingomyelin (SM) levels also appear to be important in mediating inflammation and atherosclerosis (11, 27, 34). However, few *in vivo* studies have been conducted to investigate the functions of these two metabolism-related sphingolipids separately, since animal models are lacking.

The biochemical synthesis of SM occurs through the actions of SPT, 3-ketosphinganine reductase, ceramide synthase, dihydroceramide desaturase, and sphingomyelin synthase (SMS) (36). Mammalian SPT contains two subunits, Sptlc1 and Sptlc2, encoding 53- and 63-kDa proteins, respectively (13, 64). These subunits are homologous, sharing roughly 20% sequence identity (13, 64), and form a heterodimer. A third subunit, Sptlc3, has also been reported (19), but its function remains to be elucidated. Recently, the discovery of two proteins, ssSPTa and ssSPTb, was reported. Each substantially enhances the activity of mammalian SPT, expressed in either yeast or mammalian cells, and therefore defines an evolutionarily conserved family of low-molecular-weight proteins that participate in sphingolipid biosynthesis (12).

The SMS gene family has three members, SMS1, SMS2, and SMSr (SMS-related proteins). SMS is the last enzyme for SM biosynthesis. SMS, utilizing ceramide as one of the substrates to produce SM, sits at the crossroads of the biosynthesis of these sphingolipids (36). SMS1 is found in the *trans*-Golgi apparatus, while SMS2 predominantly appears in plasma membranes (20, 66). We and other investigators have shown that SMS1 and -2 expression positively correlates with levels of cellular SM, as well as SM in lipid rafts (32, 39, 60) and negatively correlates with cellular ceramide levels (39, 60). SMSr, the third member of the gene family, has no SMS activity but catalyzes the synthesis of the SM analogue ceramide phosphoethanolamine (CPE) in the endoplasmic reticulum lumen (20, 59).

The interaction of SM, cholesterol, and glycosphingolipid drives the formation of plasma membrane rafts (51). As much as 70% of all cellular SM may be found in these rafts (32). A general consensus has developed over the last few years that

* Corresponding author. Mailing address: Department of Cell Biology, SUNY Downstate Medical Center, 450 Clarkson Ave. Box 5, Brooklyn, NY 11203. Phone: (718) 270-6701. Fax: (718) 270-3732. E-mail: xjiang@downstate.edu.

† Zhiqiang Li, Hongqi Zhang, and Jing Liu made equal contributions to this work.

▽ Published ahead of print on 15 August 2011.

the rafts represent signaling microdomains. Rafts containing the caveolin proteins manifest a unique flask-shaped structure and may possess different properties from those lacking caveolin (5, 46).

Lipid raft alterations could affect insulin signaling. It has been suggested that lipid rafts play an important role in the pathogenesis of insulin resistance (61). Indeed, disruption of caveolae in cultured cells by cholesterol extraction with β-cyclodextrin results in progressive inhibition of tyrosine phosphorylation of IRS-1, as well as reduced activation of glucose transport in response to insulin (43). Glycosphingolipids are also known to be structurally and functionally important components in the lipid rafts, possibly blocking tyrosine phosphorylation of the insulin receptor and downstream signaling (31). Pharmacological inhibition of glycosphingolipid synthesis results in markedly improved insulin sensitivity in rodent models of insulin resistance (2). A deficiency of GM3 ganglioside (a key glycosphingolipid in the rafts) enhanced insulin receptor tyrosine phosphorylation (67), and GM3 was able to dissociate the insulin receptor/caveolin-1 complex, thus causing insulin receptor dysfunctionality (28). Since SM is one of the major components within membrane lipid rafts, it is conceivable that diminishing SM in the plasma membranes could have an important impact on insulin signaling. One study (17) reported that treatment with myriocin, an SPT inhibitor, diminished *de novo* sphingolipid biosynthesis and ameliorated glucocorticoid-, saturated fat-, and obesity-induced insulin resistance.

In this study, we have utilized a gene knockout approach to study the relationship between *de novo* SM biosynthesis and insulin sensitivity.

MATERIALS AND METHODS

Mice and diet. *Sptlc2* heterozygous (*Sptlc2*$^{+/-}$) knockout (KO) and *Sms2* male mice were created in our laboratory (11, 15, 34). These and their controls were littermates or had the same genetic background. The groups of mice (at age 12 weeks) were fed either rodent chow or a high-fat and high-caloric diet (5,286 kcal kg of body weight^{-1}; D12331; Research Diets, Inc.) for 16 weeks to induce obesity (53). All procedures and protocols involving the use of animals were approved by the SUNY Downstate Medical Center Animal Care and Use Committee.

Monitoring food consumption. Groups of 10 wild-type (WT) and 10 *Sptlc2*$^{+/-}$ mice, or 10 WT and 10 *Sms2* KO mice, were utilized, with two housed in each cage. Food consumption was monitored by weighing food every day for 10 days. Consumption was recorded as g of food/g of body weight/day.

Lipid analysis by MS. Plasma and tissue ceramide, dihydroceramide, sphingosine, sphingosine-1-phosphate, sphingomyelin, glucosylceramide, GM3, and phosphatidylcholine were measured as previously described via mass spectrometry (MS) (15, 56).

Tyrosine phosphorylation of the insulin receptor. Experiments were carried out in mice fasted for 14 h. Insulin (5 units/kg of body weight; Sigma) was administered intraperitoneally (i.p.). Then, 30 min after injection, the liver, hind limb muscles, and adipose tissues (epididymal) were removed. The tissues were homogenized with lysis buffer (phosphate-buffered saline [PBS; pH 7.4], 1% Nonidet P-40, 0.5% sodium adeoxycholate, 0.1% SDS, 1 mM phenylmethylsulfonyl fluoride [PMSF], 10 mM sodium orthovanadate, 3 μg/ml aprotinin). The supernatant was precleaned by addition of protein A/G-agarose beads (sc-2003; Santa Cruz Biotechnology) at 4°C for 30 min. The solution was then spun, and the supernatant was treated with phosphorylation antibody plus agarose beads [p-Tyr(Py20)AC; sc-508AC; Santa Cruz Biotechnology] at 4°C overnight. Immunoprecipitated samples were subjected to Western blotting and probed with anti-insulin receptor β-subunit antibody. Blots were developed by chemiluminescence detection (ECL; Amersham Pharmacia). For total insulin receptor Western blotting, tissue homogenates (50 μg protein) were subjected directly to SDS-PAGE and then transferred to nitrocellulose membranes. The blots were probed sequentially, first with an anti-insulin receptor β-subunit antibody (Santa Cruz Biotechnology) and then with a tubulin or β-actin antibody (Santa Cruz Biotechnology).

Phosphorylation of Akt. Tissue homogenates (50 μg protein) were subjected to Western blotting. The blots were probed sequentially, first with an anti-phospho-Akt antibody (Ser-473; Cell Signaling) and then with an anti-Akt antibody (Cell Signaling).

Immunohistochemistry for GLUT4. Muscle and adipose tissue cryosections (10 μm) were fixed with 4% paraformaldehyde and blocked with 10% goat serum in PBS. Subsequently, sections were incubated for 1 h in primary antibodies (Abcam Inc.) to glucose transporter 4 (GLUT4), followed by incubation with the Alexa Fluor 488 goat anti-rabbit secondary antibody (Invitrogen). After washing in PBS, the sections were examined by fluorescence microscopy (Nikon).

Uptake of glucose. Mice fasted for 16 h and their control littermates were injected intravenously with 1×10^6 dpm of 2-deoxy-D-[^{3}H]glucose (Amersham). Blood was collected after 60 min. Tissues were excised, and accumulated radioactivity for 2-deoxy-D-[^{3}H]glucose was measured. Amounts of glucose injected were adjusted by plasma radioactivity counts at 60 s after each injection and were compared with plasma counts at the end of the experiments.

Lysenin treatment and cell mortality measurement. Primary hepatocytes were isolated as described elsewhere (26). The cells were incubated with 100 ng/ml lysenin for 2 h. Cell viability was measured using the WST-1 cell proliferation reagent, according to the manufacturer's instructions (Roche).

Glucose, insulin, and pyruvate tolerance tests. Glucose, insulin; or pyruvate tolerance tests were performed on fasted mice (13 to 15 h) via i.p. injections of glucose (2 g of glucose per kg of body weight) or insulin (0.75 units of insulin per kg of body weight) or pyruvate dissolved in saline (2 g of pyruvate per kg of body weight). For the glucose and pyruvate tolerance tests, blood glucose values were measured immediately before and 15, 30, 60, and 120 min after glucose injection. For the insulin tolerance test, blood glucose levels were measured immediately before and 15, 30, and 60 min after insulin injection.

Plasma and tissue free fatty acid measurements. Plasma free fatty acid was measured by using a Wako Diagnostics kit according to the manufacturer's protocol.

Liver lipid raft isolation. Liver lipid rafts were isolated, using reported protocols (10, 40). Briefly, 0.1 g mouse liver was homogenized in 1.5 ml of 0.5 M Na_2CO_3 (pH 11), containing protease inhibitors. The homogenates were centrifuged (1,300 × *g*, 5 min) to pellet cellular debris and nuclei. One milliliter of the postnuclear supernatant was then adjusted to 45% sucrose by addition of 1 ml of 90% sucrose, 50 mM HEPES (pH 6.5), and 150 mM NaCl. A discontinuous sucrose gradient was formed by overlaying this solution with 6 ml of 35% sucrose and 3.5 ml of 5% sucrose, both in the same buffer, containing 0.25 M Na_2CO_3, and this mixture was centrifuged at 38,000 rpm for 18 h in an SW41 rotor (Beckman). Fractions from top to bottom (1 ml each) were collected. Lyn kinase and caveolin-1 were used to locate the raft fractions.

Measurement of beta cell proliferation rate and relative mass. Mice were perfused through the heart with 4% paraformaldehyde buffered to pH 7.4 with 0.1 M PBS. The fixed tissues were infiltrated overnight in 30% sucrose and mounted in embedding matrix (Lipshaw Co., Pittsburgh, PA), and 20-μm cryostat sections were collected onto gelatin-coated slides. Immunostaining techniques have been previously described (33, 62). For proliferation studies, sections were immunostained for visualization of the proliferation marker Ki57 and insulin (IN). The rate of proliferation was defined as the number of Ki67$^+$ IN$^+$ cells/total number of IN$^+$ cells scored. Results are expressed as the mean ± standard error of the mean (SEM). At least 6,000 IN$^+$ cells were scored/mouse from 3 mice per line.

Exogenous sphingomyelin and ceramide supplementation. Sphingomyelins (S7004; Sigma) were dissolved in absolute ethanol, and ceramides ($C_{16:0}$; 860516P; Avanti) were dissolved in ethanol-dodecane (98/2, vol/vol). HepG2 cells were incubated with exogenous 0, 10, 20, 40 μM sphingomyelins or with 0, 10, 20, or 40 μM exogenous ceramides for 5 h, the cells were treated with 100 nM insulin for 10 min, and Akt phosphorylation in whole-cell homogenates was measured.

Statistical analysis. Each experiment was conducted at least three times. Data are typically expressed as means ± standard deviations (SD). Data between two groups were analyzed by unpaired, two-tailed Student's *t* test.

RESULTS

***Sptlc2* heterozygous deficiency protects mice from insulin resistance.** In this study, we utilized *Sptlc2* heterozygous KO (*Sptlc2*$^{+/-}$) mice to examine the relationship between SPT activity and insulin sensitivity. The liver, skeletal muscles, and

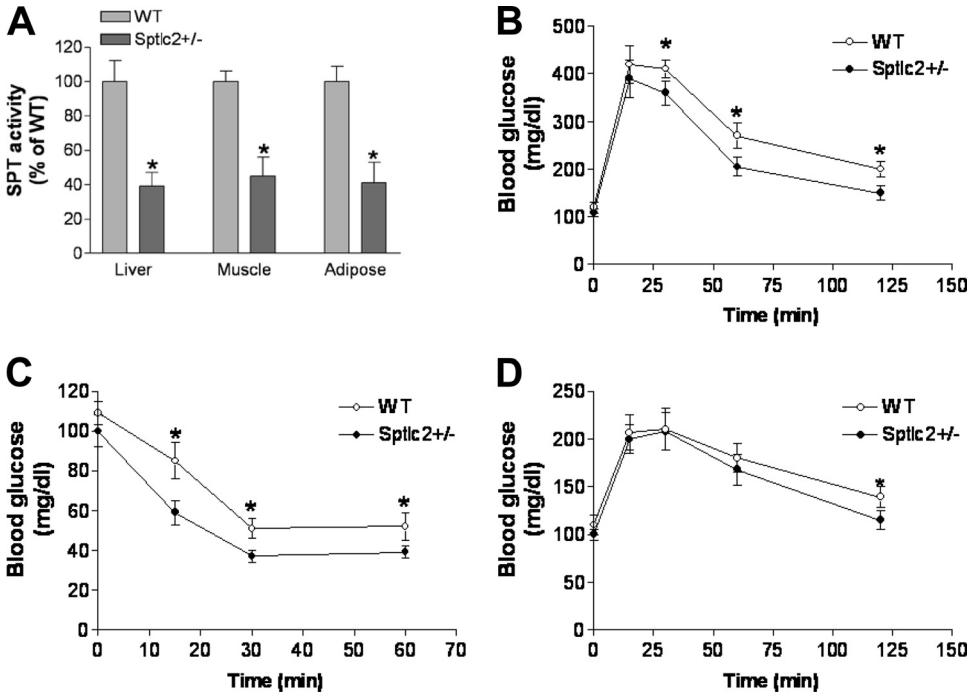

FIG. 1. Effects of heterozygous *Sptlc2* deficiency on glucose, insulin, and pyruvate tolerance tests. Mice were on a chow diet. (A) Tissue SPT activity measurement in *Sptlc2*$^{+/-}$ and WT mice; (B) Glucose tolerance test; (C) insulin tolerance test; (D) pyruvate tolerance test. Values are means ± SD ($n = 10$). *, $P < 0.01$.

adipose tissues are three major tissues involved in insulin action. Previously, we showed that liver SPT activity in *Sptlc2*$^{+/-}$ mice is 60% lower than in controls (15). In this study, we confirmed this observation. Moreover, we found that SPT activities in skeletal muscles and adipose tissues were also significantly decreased in *Sptlc2*$^{+/-}$ mice compared with controls (53 and 59%, respectively) (Fig. 1A). No differences were found between WT and *Sptlc2*$^{+/-}$ mice in body weight (25 ± 2 versus 26 ± 3 g at age 12 weeks) or food consumption (99 ± 20 versus 106 ± 26 g/kg/day) on a chow diet.

We utilized enzymatic assays to measure plasma lipid levels in these animals and found that *Sptlc2* deficiency significantly decreased free fatty acids and triglycerides (44% and 32%, respectively) (Table 1).

We used liquid chromatography-tandem MS (LC-MS/MS) to measure sphingomyelin, ceramide, sphinganine, sphinganine-1-phosphate, sphingosine, sphingosine-1-phosphate, hydroceramide, glucosylceramide, GM3, diacylglycerol, and phosphatidylcholine levels in the plasma, liver, adipose tissues, and muscle. We did not find significant changes of these lipids, except that both liver ceramide and adipose tissue glucosylceramide were significantly increased (Table 2).

TABLE 1. Mouse plasma lipid and free fatty acid measurements[a]

Mouse diet and genotype	FFA (mM)	TG (mg/dl)	SM (mg/dl)	Chol (mg/dl)	PC (mg/dl)
Chow					
WT	0.9 ± 0.3	75 ± 13	22 ± 3	110 ± 15	112 ± 13
Sptlc2$^{+/-}$	0.5 ± 0.1*	51 ± 10**	19 ± 2	109 ± 36	118 ± 35
High fat					
WT	1.6 ± 0.2	109 ± 16	35 ± 2	190 ± 19	201 ± 21
Sptlc2$^{+/-}$	1.2 ± 0.1**	81 ± 12*	28 ± 2*	198 ± 11	198 ± 25

[a] Values are means ± SD ($n = 10$). *, $P < 0.05$; **, $P < 0.01$ compared to WT. FFA, free fatty acids; TG, triglycerol; Chol, cholesterol.

We performed glucose tolerance tests in fasting animals, and we found that the *Sptlc2*$^{+/-}$ mice had an improved glucose tolerance (Fig. 1B). Blood glucose levels at all time points after glucose injection (except 15 min) were significantly different between the two groups ($P < 0.01$). We also carried out insulin tolerance tests on these animals. Fasting *Sptlc2*$^{+/-}$ and WT mice were challenged with insulin, and their blood glucose levels were monitored for 60 min. As shown in Fig. 1C, *Sptlc2*$^{+/-}$ mice had significantly less glucose in the circulation than WT animals after insulin treatment, indicating that *Sptlc2* heterozygous deficiency increases insulin sensitivity. We probed whether *Sptlc2* partial deficiency induces impairment of gluconeogenesis, which could contribute to the pathophysiological production and clearance of glucose. To this end, the administration of the gluconeogenic substrate precursor pyruvate (pyruvate tolerance test) showed that there was no difference in glucose production in *Sptlc2*$^{+/-}$ mice (Fig. 1D). Hence, partial loss of function of *Sptlc2* had no impact on the gluconeogenesis pathway. However, upon glucose production (30 min), the clearance rates of glucose were again significantly faster in *Sptlc2*$^{+/-}$ than in WT mice (Fig. 1D), confirming a promotion in glucose clearance.

We placed *Sptlc2*$^{+/-}$ and WT mice on a high-fat, high-caloric diet for 16 weeks in an attempt to induce obesity and insulin resistance (53). As shown in Fig. 2A, starting from week 4, *Sptlc2*$^{+/-}$ mice gained significantly less body weight than WT animals. Moreover, *Sptlc2*$^{+/-}$ mice had significantly less adi-

TABLE 2. Mouse plasma and tissue lipid analysis by LC-MS/MS[a]

Compartment and lipid	Chow diet		High-fat diet	
	WT	*Sptlc2*$^{+/-}$	WT	*Sptlc2*$^{+/-}$
Plasma				
Sph (ng/ml)	30 ± 6	33 ± 7	41 ± 11	45 ± 10
S1P (ng/ml)	262 ± 39	227 ± 21	401 ± 36	293 ± 27*
Sa (ng/ml)	36 ± 8	23 ± 8	26 ± 5	24 ± 3
Sa1P (ng/ml)	111 ± 16	86 ± 19	205 ± 57	105 ± 21*
DAG (ng/ml)	1,508 ± 146	1,346 ± 119	8,129 ± 1393	7,250 ± 1480
SM (nmol/ml)	117 ± 26	96 ± 15	203 ± 16	175 ± 12*
PC (nmol/ml)	1,752 ± 254	1,405 ± 383	5,289 ± 655	4,713 ± 383
Cer (ng/ml)	967 ± 99	813 ± 78	3,235 ± 381	1,569 ± 233*
DHCer (ng/ml)	130 ± 26	105 ± 20	440 ± 50	219 ± 28*
GlyCer (ng/ml)	5,307 ± 1212	3,354 ± 679	23,450 ± 5,210	19,569 ± 2,135
GM3 (ng/ml)	212 ± 29	182 ± 30	397 ± 51	366 ± 36
Liver				
Sph (ng/mg)	2.09 ± 0.31	1.96 ± 0.33	4.05 ± 0.61	3.59 ± 0.41
Sa (ng/mg)	0.42 ± 0.02	0.34 ± 0.08	1.17 ± 0.03	1.09 ± 0.05
DAG (ng/mg)	553 ± 78	486 ± 81	1351 ± 395	1297 ± 379
SM (nmol/mg)	0.74 ± 0.16	0.66 ± 0.15	1.10 ± 0.14	1.19 ± 0.05
PC (nmol/mg)	18.12 ± 6.60	19.51 ± 3.08	22.42 ± 1.50	23.59 ± 0.86
Cer (ng/mg)	133.7 ± 21.2	154.8 ± 18.3*	143.7 ± 12.3	185.5 ± 15.7*
DHCer (ng/mg)	17.4 ± 2.4	21.1 ± 3.5	17.8 ± 3.3	20.3 ± 1.7
GlyCer (ng/mg)	105.0 ± 19.3	82.9 ± 22.2	77.9 ± 15.6	79.7 ± 16.3
GM3 (ng/mg)	10.9 ± 1.3	9.5 ± 1.2	7.1 ± 1.1	7.9 ± 0.8
Adipose tissue				
Sph (ng/mg)	0.07 ± 0.01	0.09 ± 0.01	0.12 ± 0.00	0.09 ± 0.00
Sa (ng/mg)	0.14 ± 0.00	0.12 ± 0.01	0.15 ± 0.01	0.15 ± 0.01
SM (nmol/mg)	0.32 ± 0.03	0.36 ± 0.04	0.28 ± 0.05	0.32 ± 0.06
PC (nmol/mg)	1.09 ± 0.10	1.21 ± 0.29	1.11 ± 0.31	1.01 ± 0.21
Cer (ng/mg)	8.96 ± 0.77	8.77 ± 0.81	9.45 ± 1.10	8.88 ± 0.91
GlyCer (ng/mg)	0.70 ± 0.06	1.42 ± 0.31*	3.27 ± 0.41	2.95 ± 0.36
GM3 (ng/mg)	0.37 ± 0.09	0.58 ± 0.11	0.40 ± 0.06	0.30 ± 0.10
Muscle				
Sph (ng/mg)	0.10 ± 0.02	0.09 ± 0.01	0.14 ± 0.04	0.11 ± 0.03
Sa (ng/mg)	0.11 ± 0.03	0.10 ± 0.01	0.13 ± 0.02	0.12 ± 0.02
SM (nmol/mg)	0.32 ± 0.08	0.28 ± 0.05	0.31 ± 0.08	0.35 ± 0.06
PC (nmol/mg)	8.03 ± 1.15	7.84 ± 1.66	5.59 ± 1.12	7.30 ± 1.75
Cer (ng/mg)	25.41 ± 4.33	25.11 ± 4.91	28.50 ± 3.82	27.75 ± 2.30
GlyCer (ng/mg)	46.51 ± 7.11	38.33 ± 6.91	39.10 ± 5.59	48.39 ± 6.99
GM3 (ng/mg)	10.60 ± 2.13	9.93 ± 1.48	9.05 ± 1.59	8.46 ± 1.36

[a] Values are means ± SD ($n = 5$). *, $P < 0.05$ compared to WT. Sph, sphingosine; S1P, sphingosine-1-phosphate; Sa, sphinganine; Sa1P, sphinganine-1-phosphate; DAG, diacylglycerol; Cer, ceramide; DHCer, dihydroceramide; Glycer, glucosylceramide.

pose tissue (as a percentage) than WT animals (Fig. 2B). However, there was no significant difference in food consumption between the two groups (116 ± 31 versus 109 ± 21 g/kg/day).

It has been reported that smaller adipocytes are usually accompanied by increased insulin sensitivity (70). To determine whether this is the case in *Sptlc2*$^{+/-}$ adipocytes, we dissected the adipose tissues, staining them with hematoxylin and eosin. The images were analyzed to determine the cross-sectional surface area of each adipocyte. *Sptlc2*$^{+/-}$ mice had a greater number of small adipocytes than WT. This difference in frequency distribution was reflected in a 40% decrease in mean surface area of adipocytes from *Sptlc2*$^{+/-}$ mice (Fig. 2C and D).

We also utilized enzymatic assays to measure plasma lipid levels in these animals and found that *Sptlc2* deficiency significantly decreased plasma SM, free fatty acid, and triglyceride levels (20%, 25%, and 26%, respectively), but not cholesterol or phosphatidylcholine levels (Table 1).

We used LC-MS/MS to measure plasma sphingolipids as well as diacylglycerol and phosphatidylcholine levels. As expected, plasma SM, sphinganine-1-phosphate, sphingosine-1-phosphate, ceramide, and hydroceramide were significantly decreased but diacylglycerol, glucosylceramide, and GM3 were not (Table 2).

We likewise assayed these lipid levels in the liver. Unexpectedly, when the animals were on a high-fat diet, liver ceramide levels were significantly increased in *Sptlc2*$^{+/-}$ mice, compared with controls. We found no changes in other lipids (Table 2). We then measured sphingomyelinase (SMase) and SMS activity, and we found that liver SMase but not SMS activity was increased in *Sptlc2*$^{+/-}$ mice, compared with controls (39%; $P < 0.05$), suggesting that increased SMase activity might be responsible for the increased liver ceramide levels. We likewise

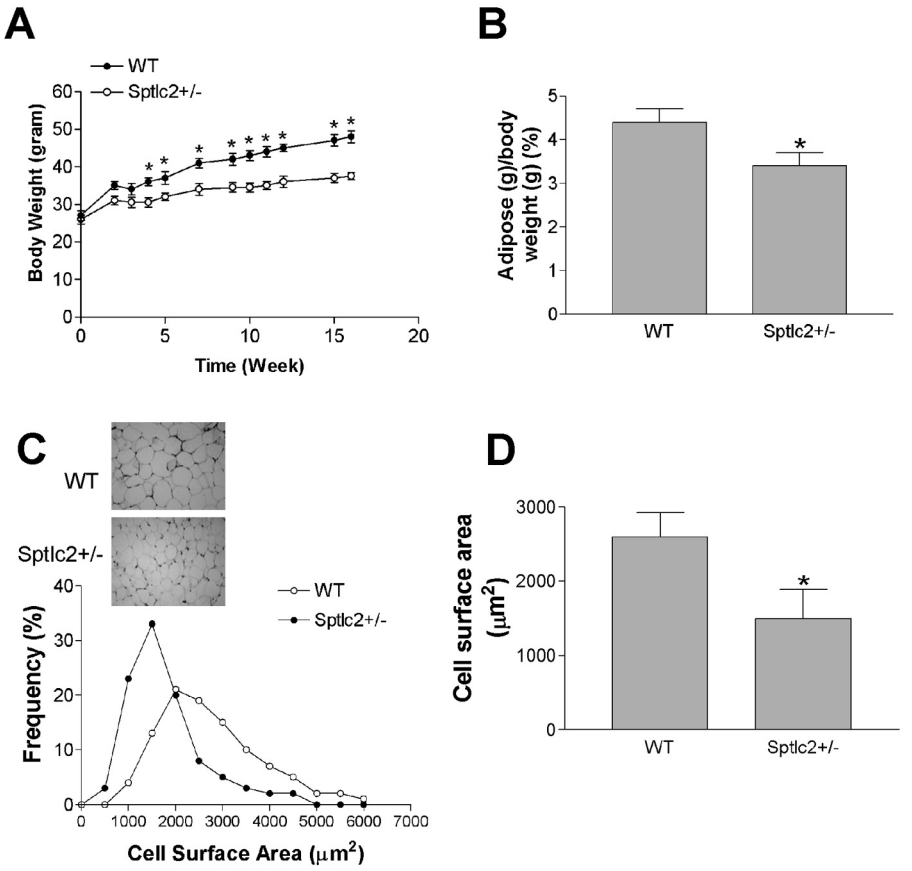

FIG. 2. Effects of heterozygous *Sptlc2* deficiency on dietary-induced body weight gain and adipose tissues. Mice were fed a high-fat, high-caloric diet for 16 weeks. (A) Quantitative display of body weight gain in *Sptlc2*$^{+/-}$ and WT mice. (B) Adipose tissue/body weight ratios. (C) Decrease of adipocyte size in *Sptlc2*$^{+/-}$ mice. Hematoxylin- and eosin-stained sections of adipose tissues from WT and *Sptlc2*$^{+/-}$ mice are shown. Images were captured at 10× magnification. The frequency distribution shows adipocyte cell surface areas from five WT and five *Sptlc2*$^{+/-}$ mice. More than 200 cells were measured for each mouse. The distribution includes 1,115 cells from WT and 1,207 from *Sptlc2*$^{+/-}$ mice. (D) Mean surface area of adipocytes. Values are means ± SD ($n = 10$). *, $P < 0.01$.

measured all these lipids in the adipose tissues and skeletal muscles, and we found that there were no significant differences between WT and *Sptlc2*$^{+/-}$ animals on the high-fat diet (Table 2).

We then measured plasma leptin and adiponectin levels, since both are related to insulin sensitivity (57, 65), and we found no significant differences between *Sptlc2*$^{+/-}$ and WT mice (data not shown).

We next performed glucose tolerance tests in fasting animals, and we found that WT mice on a high-fat, high-caloric diet were glucose intolerant, as evidenced by a decreased ability to lower their blood glucose, while the *Sptlc2*$^{+/-}$ animals were significantly better at doing so (Fig. 3A). We also carried out insulin tolerance tests on these animals. As shown in Fig. 3B, *Sptlc2*$^{+/-}$ mice had significantly less glucose in the circulation than WT animals after insulin treatment, indicating that *Sptlc2* heterozygous deficiency increases insulin sensitivity. Moreover, as shown in Fig. 3C, *Sptlc2*$^{+/-}$ mice had significantly lower fasting and fed insulin levels. Furthermore, we measured insulin levels after glucose injection, and we found that *Sptlc2*$^{+/-}$ mice had less insulin than WT animals (Fig. 3D).

To ascertain whether the mutation affected the pancreatic islets, we compared the rate of beta cell proliferation and beta cell mass in *Sptlc2*$^{+/-}$ and WT mice. As illustrated in Fig. 4A and B, the beta cell mass was similar in *Sptlc2*$^{+/-}$ and WT animals. Moreover, the rate of proliferation, calculated as the percentage of insulin-positive cells expressing the proliferation marker Ki67, was comparable in both lines (Fig. 4C and D). These findings indicate that the increased insulin sensitivity observed in *Sptlc2*$^{+/-}$ mice is not due to differences in the number of beta cells.

To gain mechanistic insight into the increase in insulin sensitivity associated with heterozygous *Sptlc2* deficiency, we investigated the phosphorylation-mediated activation of the insulin receptor that occurs after interaction with circulating insulin. After injecting it, we found that *Sptlc2* deficiency significantly enhanced tyrosine-phosphorylated insulin receptor levels in mouse liver, skeletal muscles, and adipose tissues, while total insulin receptor levels were unchanged (Fig. 5A and B). This was also true for Akt phosphorylation, one of the downstream targets of insulin receptor activation (Fig. 5C and D). We performed the same experiments on *Sptlc2*$^{+/-}$ and WT mice on a chow diet, finding that, after insulin stimulation, *Sptlc2* deficiency also caused significantly increased phosphorylated insulin receptor levels (Fig. 6A and B) and Akt levels (Fig. 6C and D) in mouse liver and adipose tissues, but not in skeletal muscles.

We next sought to measure GLUT4 levels in adipose tissues and skeletal muscles by using immunohistochemistry, since GLUT4 is one of the known genes downstream of the insulin

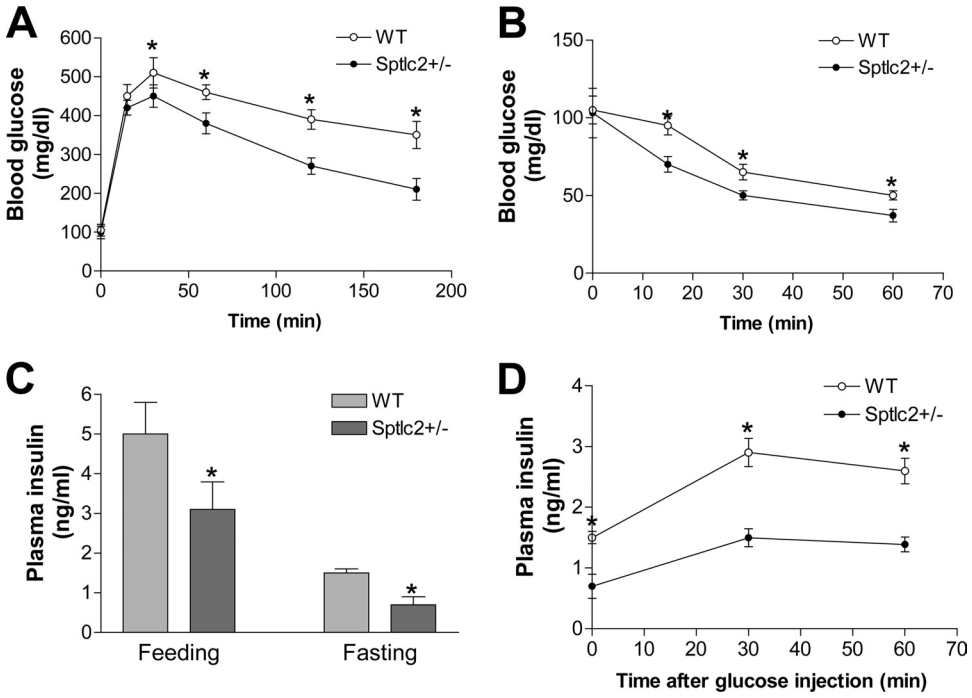

FIG. 3. Effects of heterozygous *Sptlc2* deficiency on glucose tolerance, insulin tolerance, and plasma insulin levels. Mice were fed a high-fat, high-calorie diet for 16 weeks. (A) Glucose tolerance test; (B) insulin tolerance test; (C) fasting and feeding plasma insulin level measurements; (D) plasma insulin levels after glucose injection. Values are means ± SD ($n = 10$). *, $P < 0.01$.

receptor and Akt (3). We expected that increased insulin receptor activation would increase surface expression of GLUT4 in both adipose tissues and skeletal muscles. Indeed, after insulin stimulation, *Sptlc2* deficiency induced significantly more GLUT4 immunostaining in the plasma membranes of adipocytes and muscle cells (Fig. 5E), confirming the enhancement of insulin signaling.

To examine the effects of increased GLUT4 levels in

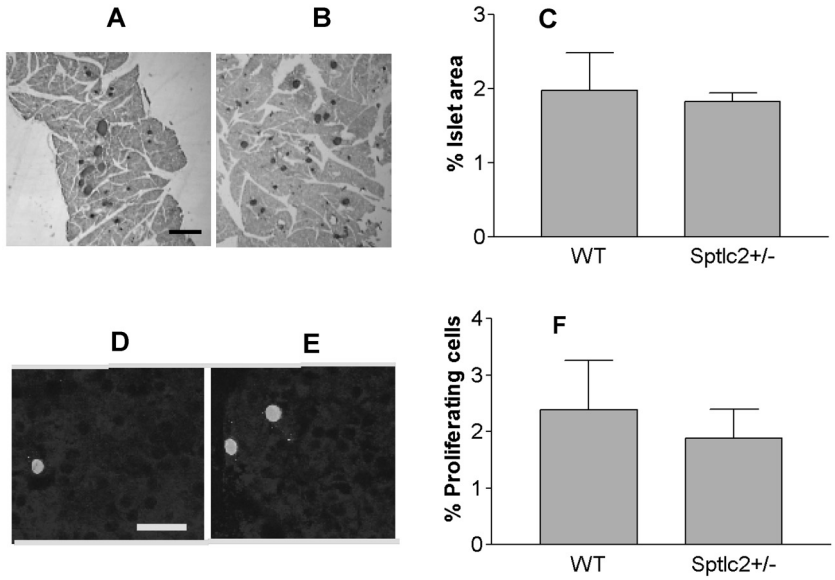

FIG. 4. Heterozygous *Sptlc2* deficiency has no effect on beta cell mass and proliferation. (A and B) Photomicrographs illustrating sections of the pancreas of WT (A) and *Sptlc2* KO (B) mice immunostained for visualization of insulin, using diaminobenzidine as a substrate. Islets were visualized by the brown reaction product on beta cells. Similarly processed sections were used for morphometric analysis of beta cell mass. Bar, 150 μm. (C) Histogram analyzing the presence of similar beta cell mass in *Sptlc2* KO and littermate controls. Beta cell mass was determined as described in Materials and Methods ($n = 3$, with at least 10 fields per mouse/strain evaluated). (D and E) Photomicrographs illustrating beta cells in a section of WT (D) and *Sptlc2* KO (E) that were processed for visualization of insulin and the proliferation marker Ki67. Note that the cell indicated with green is IN^+ $Ki67^+$. Bar, 20 μm. (F) Histogram documenting the percentage of proliferating (IN^+ $Ki67^+$) cells per total number of IN^+ cells scored. At least 6,000 IN^+ cells were scored per mouse, and 3 mice per strain were analyzed.

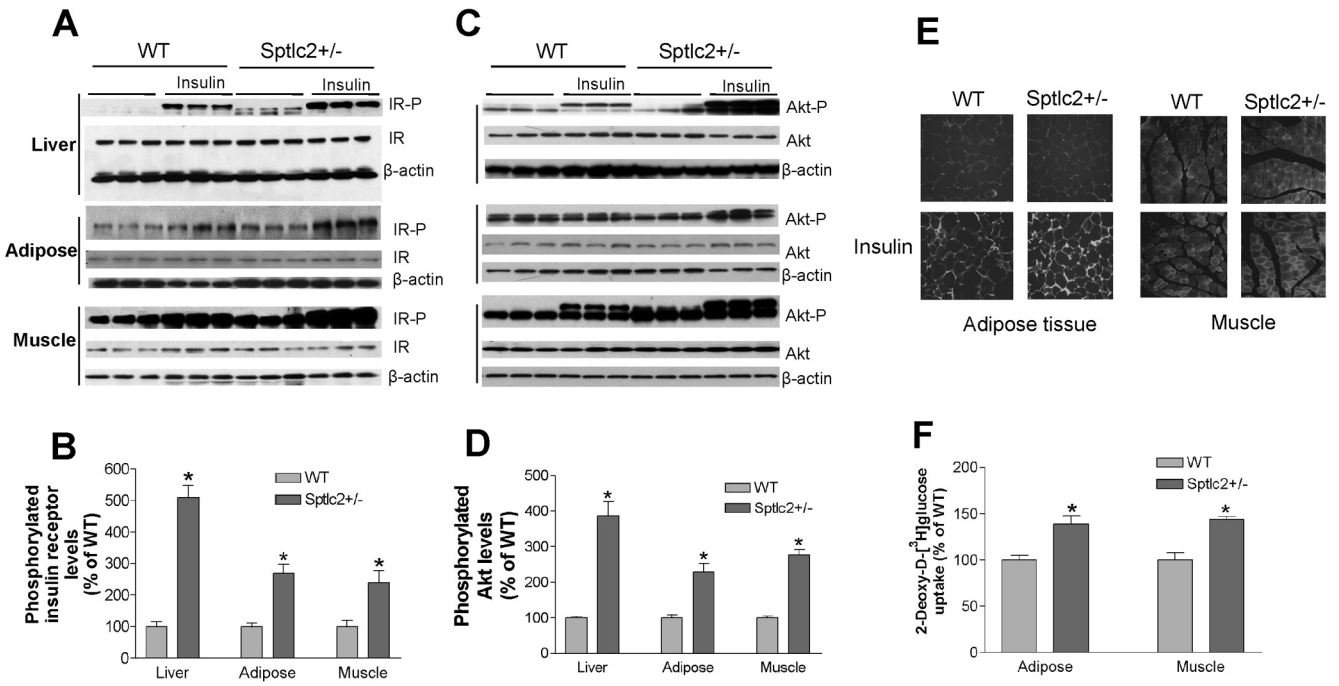

FIG. 5. Effects of heterozygous *Sptlc2* deficiency on insulin signaling. Mice were fed a high-fat, high-caloric diet for 16 weeks. (A) Phosphorylated insulin receptor measurements by Western blotting. IR-P, phosphorylated insulin receptor; IR, total insulin receptor; β-actin, loading control. (B) Quantitative display of phosphorylated insulin receptor in liver, adipose tissues, and muscles. (C) Phosphorylated Akt measurements by Western blotting. Akt-P, phosphorylated Akt. (D) Quantitative display of phosphorylated Akt in liver, adipose tissues, and muscles. Values are means ± SD ($n = 6$). *, $P < 0.01$. (E) GLUT4 immunostaining. Muscle and adipose tissue cryosections (10 μm) were fixed with 4% paraformaldehyde and incubated with a primary antibody to GLUT4. The appropriate secondary antibody conjugated with fluorescein Cy3 was used to detect the signal. The sections were examined by fluorescence microscopy (Nikon). The results shown are representative of three independent experiments. (F) Glucose uptake measurement. Mice fasted for 16 h were injected intravenously with 1×10^6 dpm of 2-deoxy-D-[^{3}H]glucose. Blood was collected after 60 min. Tissues were then excised, and accumulated radioactivity of 2-deoxy-D-[^{3}H]glucose was measured. The amount of glucose injected was adjusted based on plasma radioactivity counts at 60 s after each injection and was compared with plasma counts at the end of the experiments. Tissue uptake for *Sptlc2*$^{+/-}$ mice was compared with uptake of WT littermates. Values are means ± SD ($n = 10$). *, $P < 0.05$.

Sptlc2$^{+/-}$ mice, we injected 2-deoxy-D-[^{3}H]glucose intravenously (i.v.) and measured its uptake rate in adipose tissues and skeletal muscles. We found that in heterozygous *Sptlc2*-deficient mice, both skeletal muscles and adipose tissues took up significantly more 2-deoxy-D-[^{3}H]glucose than controls (Fig. 5F).

Lipid rafts play a major role in insulin receptor activation (22, 28, 67). Like GM3, plasma membrane lipid raft SM levels may relate to insulin sensitivity. In order to measure SM in plasma membranes, we employed lysenin, an SM-specific cytotoxin. Lysenin recognizes SM only when it has formed aggregates or microdomains in the plasma membranes and has subsequently lysed the cells (23). Lysenin-mediated cell mortality can indirectly reflect SM levels in plasma membranes (2, 11, 35). We found that *Sptlc2*$^{+/-}$ hepatocytes were significantly more resistant to lysenin-mediated cell lysis ($P < 0.01$) (Fig. 7A), suggesting that *Sptlc2*$^{+/-}$ hepatocytes had significantly less SM in the plasma membrane lipid rafts than did controls. Similar results were obtained for mice on a chow diet (data not shown).

We then investigated whether heterozygous *Sptlc2* deficiency affects insulin receptor tyrosine phosphorylation in lipid rafts. We isolated these rafts from the whole liver, using reported protocols (10, 40). Insulin receptor was found in light fractions enriched with the raft markers Lyn kinase and caveolin-1 (Fig. 7B). We measured SM levels in each fraction using our enzymatic assay (14) and found that SM levels in *Sptlc2*$^{+/-}$ hepatocyte membrane lipid rafts were indeed significantly decreased compared with controls, while there were no significant changes in nonraft regions (Fig. 7C). We pooled raft fractions (4 to 6) and nonraft fractions (10 to 12) to perform insulin receptor Western blotting. As seen in Fig. 7D and E, raft regions contained a relatively small amount of tyrosine-phosphorylated insulin receptor before insulin stimulation. The amount of these receptors in the raft regions was significantly increased after insulin stimulation in *Sptlc2*$^{+/-}$ liver compared with controls (2.8-fold; $P < 0.01$), but there were no significant changes of total insulin receptor in the raft domains (i.e., without alterations in receptor distribution or localization). These results suggest that *Sptlc2* deficiency-mediated SM depletion in plasma membrane SM-rich microdomains contributes to insulin receptor tyrosine phosphorylation of insulin.

The problem with a lysenin approach is that it cannot directly measure SM and ceramide levels. Since *Sptlc2*$^{+/-}$ mice had increased insulin sensitivity on both the chow and high-fat diet (Fig. 1 and Fig. 3), we then isolated plasma membranes with reasonable purity from mouse liver (on chow) (Fig. 7F) and measured SM and ceramide as well as other sphingolipid levels, using LC-MS/MS. We found that, in *Sptlc2*$^{+/-}$ hepatocyte membranes, SM and ceramide levels were significantly decreased but glucosylceramide levels were not (Table 3).

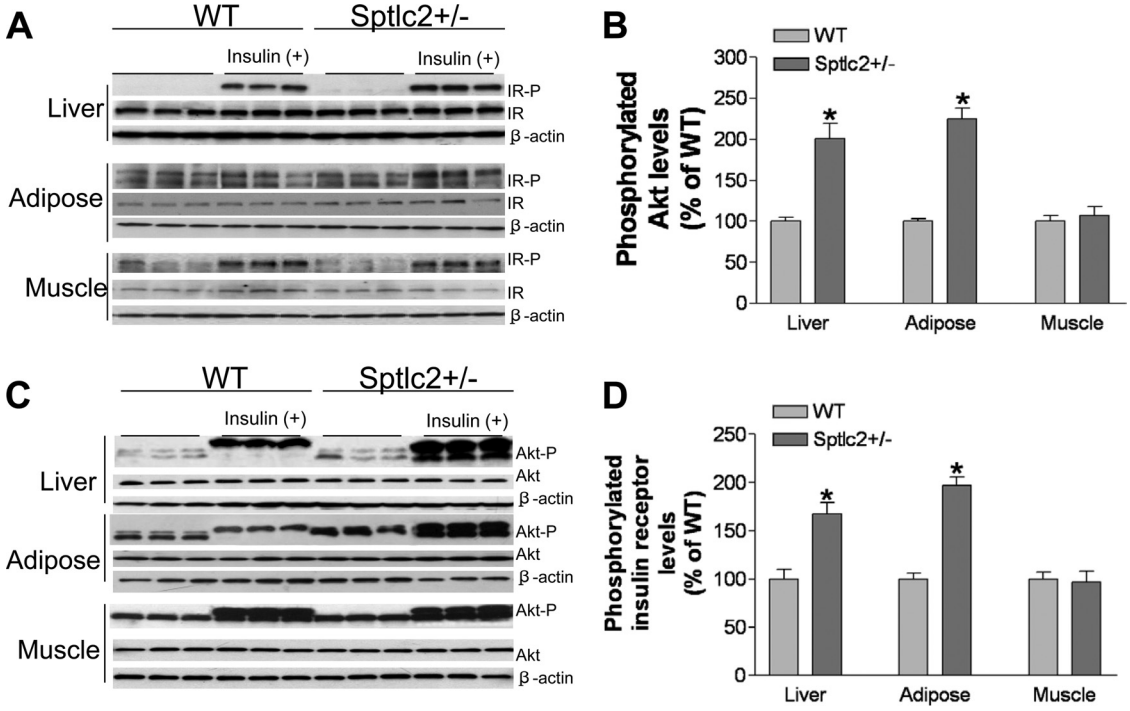

FIG. 6. Effects of heterozygous *Sptlc2* deficiency on phosphorylation of insulin receptor and Akt (on chow). Mice were fed a chow diet for 6 months. (A) Phosphorylated insulin receptor measurement. Thirty minutes after insulin treatment, the liver, hind limb muscles, and adipose tissues were removed and treated as described in Materials and Methods. The total phosphorylated proteins were immunoprecipitated with a phosphorylation antibody plus agarose beads at 4°C overnight. Immunoprecipitated samples were subjected to SDS-PAGE and then transferred to nitrocellulose membranes. Blots were probed with anti-insulin receptor β-subunit antibody. Blots were developed with a chemiluminescence detection system. IR-P, phosphorylated insulin receptor; IR, total insulin receptor; β-actin, loading control. (B) Quantitative display of phosphorylated insulin receptor levels in the liver, adipose tissues, and muscles. Displayed are means ± SD ($n = 6$). (C) Phosphorylated Akt measurements. Tissue homogenates (50 μg protein) were subjected to SDS-PAGE and then transferred to nitrocellulose membranes. The blots were probed sequentially, first with an anti-phospho-Akt antibody (Cell Signaling) and then with an anti-Akt antibody (Cell Signaling). Akt-P, phosphorylated Akt. (D) Quantitative display of phosphorylated Akt in the liver, adipose tissue, and muscle. Displayed are means ± SD ($n = 6$).

***Sms2* deficiency protects mice from insulin resistance.** We prepared sphingomyelin synthase 2 (*Sms2*) KO mice, as previously reported (11, 35, 68). We found that SMS activity was significantly decreased in liver, adipose tissues, and muscles (Fig. 8A). On a chow diet, no differences were found between WT and *Sms2* KO mice in body weight or food consumption (data not shown).

We measured sphingolipid levels in these mice, and we found that SM was significantly decreased while ceramide was increased in the liver, adipose tissues, and muscles (Table 4). Moreover, we found no changes of sphingomyelinase activity in any of these tissues (data not shown), indicating that the sphingolipid changes are *Sms2* deficiency mediated.

We also measured plasma lipid levels in these animals, and we found that *Sms2* deficiency significantly decreased plasma SM and free fatty acid levels, but not those of cholesterol, phosphatidylcholine, or triglyceride (Table 5).

We performed glucose tolerance tests in these mice under fasting conditions, and we found that *Sms2* mice performed significantly better in their ability to remove glucose from the circulation (Fig. 8B). Fasting *Sms2* KO and WT mice were also challenged with insulin, and their blood glucose levels were monitored at different time points up to 60 min. As shown in Fig. 8C, *Sms2* mice had significantly less glucose in the circulation than WT animals after insulin treatment, indicating that *Sms2* deficiency increases insulin sensitivity.

We placed *Sms2* KO and WT mice on a high-fat, high-caloric diet for 20 weeks in an attempt to induce obesity and insulin resistance (53). As shown in Fig. 9A, starting from week 5, *Sms2* KO mice gained significantly less body weight than WT animals. We performed glucose tolerance (Fig. 9B) and insulin tolerance (Fig. 9C) tests in fasting animals, and again we found that *Sms2* deficiency increased insulin sensitivity. Moreover, as shown in Fig. 9E, *Sms2* KO mice had significantly lower fasting and fed insulin levels. We also measured insulin levels after glucose injection, and we found that *Sms2* mice had less insulin than WT animals (Fig. 9F). We also performed a pyruvate tolerance test, and we did not find differences in glucose production between WT and *Sms2* KO mice (Fig. 9D). However, upon glucose production (30 min), the clearance rates of glucose were again significantly faster in *Sms2* KO mice than in WT mice. Collectively, these data suggest quite strongly that *Sms2* KO mice develop increased insulin sensitivity.

We next measured plasma membrane SM levels using lysenin analysis, and we found that *Sms2*-deficient hepatocytes resist lysenin-mediated cell lysis (Fig. 10A), which indicates that *Sms2*-deficient hepatocytes have less SM in the plasma membranes.

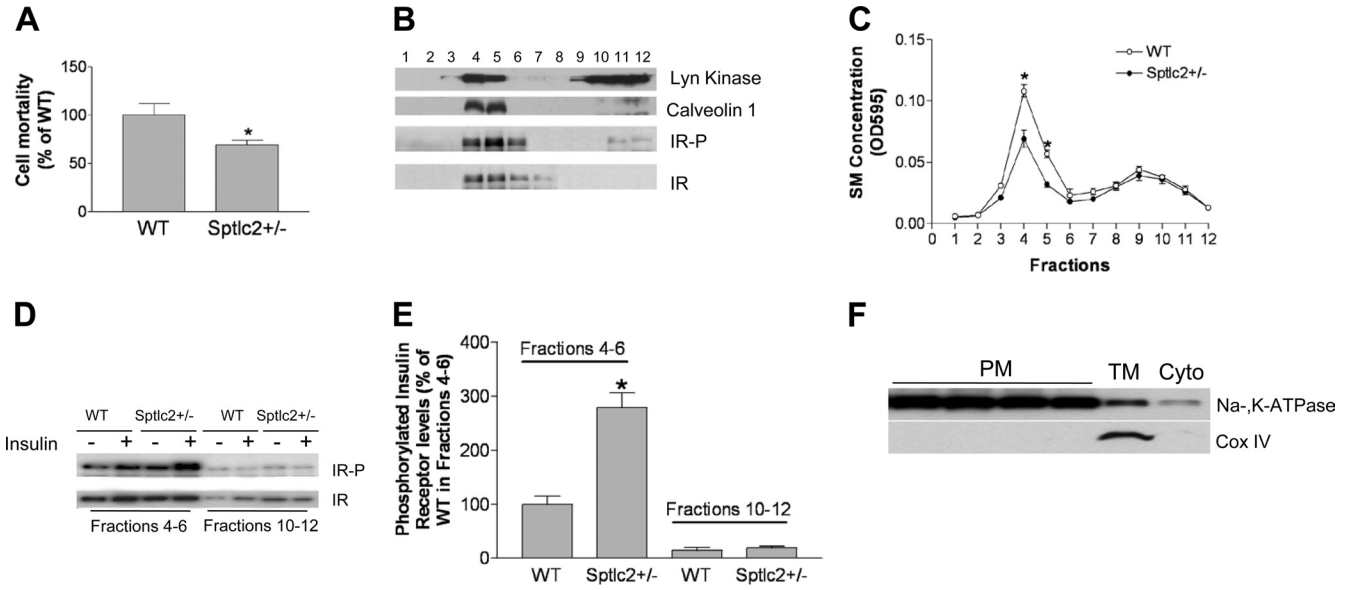

FIG. 7. Heterozygous *Sptlc2* deficiency increases the levels of phosphorylated insulin receptor in liver lipid rafts. Mice were fed a high-fat, high-caloric diet for 16 weeks. (A) Lysenin-mediated cell lysis assay. (B) Lipid raft isolation according to the method described in the text. Fractions (1 to 12) were collected from the top to the bottom after gradient centrifugation. Each fraction was used for the detection of Lyn kinase, caveolin-1, phosphorylated insulin receptor, and total insulin receptor. (C) SM measured by enzymatic assay in each fraction. (D) Fractions 4 to 6 (lipid rafts) and fractions 10 to 12 (nonrafts) were pooled. Phosphorylated insulin receptor and total insulin receptor in both rafts and nonrafts before and after insulin stimulation were detected by Western blotting. (E) Quantitative display of phosphorylated insulin receptor in the liver lipid rafts and nonrafts. (F) Mouse liver plasma membranes were isolated, and purity was determined by Western blotting of a plasma membrane marker (Na/K-ATPase) and a mitochondrial marker (Cox IV).

Since *Sms2* KO mice had increased insulin sensitivity on both the chow and high-fat diet (Fig. 8 and 9), we then isolated plasma membranes from mouse liver (on chow) and measured SM and ceramide, as well as other sphingolipid levels, using LC-MS/MS. We found that only SM levels were significantly decreased (Table 3). Other lipids, including ceramide, glycosylceramide, dihydroceramide, sphingosine, GM3, and phosphatidylcholine (PC), were not significantly changed (Table 3).

TABLE 3. Mouse liver plasma membrane lipid analysis by LC-MS/MS (on chow diet)[a]

Genotype and lipid analyzed	WT	KO
Sptlc2$^{+/-}$		
Sph (ng/mg)	16 ± 7	12 ± 1
Sa (ng/mg)	3 ± 1	2 ± 1*
PC (nmol/mg)	173 ± 41	75 ± 41*
SM (nmol/mg)	38 ± 5	18 ± 5**
Cer (ng/mg)	2,688 ± 646	1,704 ± 196*
DHCer (ng/mg)	420 ± 70	315 ± 18*
GlyCer (ng/mg)	826 ± 82	846 ± 145
GM3 (ng/mg)	399 ± 165	428 ± 60
Sms2		
Sph (ng/mg)	14 ± 7	13 ± 5
Sa (ng/mg)	5 ± 4	3 ± 1
PC (nmol/mg)	67 ± 25	49 ± 16
SM (nmol/mg)	30 ± 4	15 ± 2*
Cer (ng/mg)	2,235 ± 346	2,238 ± 570
DHCer (ng/mg)	317 ± 135	301 ± 74
GlyCer (ng/mg)	502 ± 57	558 ± 37
GM3 (ng/mg)	266 ± 50	280 ± 60

[a] Values are means ± SD. *, $P < 0.05$; **, $P < 0.01$ compared to WT. Sph, sphingosine; Sa, sphinganine; Cer, ceramide; DHCer, dihydroceramide; Glycer, glucosylceramide.

To examine the effects of *Sms2* deficiency-mediated glucose uptake, we injected 2-deoxy-D-[^{3}H]glucose (i.v.) and measured its uptake rate in adipose tissues and skeletal muscles. We found that in *Sms2*-deficient mice, both skeletal muscles and adipose tissues took up significantly more 2-deoxy-D-[^{3}H]glucose than controls (Fig. 10B).

We measured Akt phosphorylation in the liver and found that after insulin stimulation there was more phosphorylated Akt in *Sms2* KO liver homogenate than in controls (Fig. 10C and D). In general, *Sms2* KO and *Sptlc2*$^{+/-}$ mice have similar phenotypes with regard to insulin sensitivity. These results suggest that SM is potentially the principal regulator of insulin resistance in these models.

To pinpoint the hypothesis that SM affects insulin signaling, cell culture experiments in which SM levels can be modulated are needed. It has been shown that exogenously added SM significantly diminishes cholesterol efflux mediated by a lipid rafts-associated cholesterol transporter (30, 41), suggesting that the increase in SM content in the plasma membrane prevents cholesterol efflux.

We incubated HepG2 cells, a hepatoma line, with exogenous SM at 0, 10, 20, or 40 μM for 5 h. We then treated the cells with 100 nM insulin for 10 min and measured Akt phosphorylation in whole-cell homogenates. We found that Atk phosphorylation was decreased in an SM concentration-dependent fashion (Fig. 10E and F). In the same tissue culture system, we added 0, 10, 20, or 40 μM exogenous natural ceramide ($C_{16:0}$),

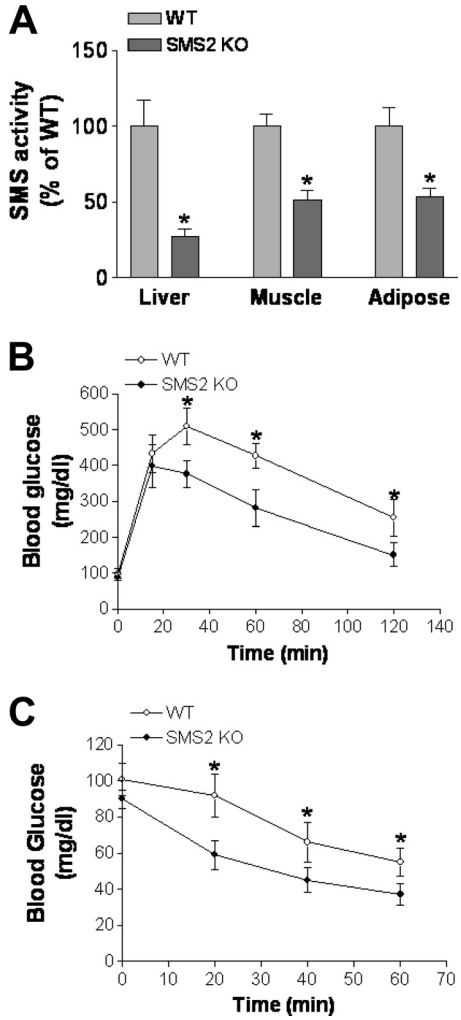

FIG. 8. Effects of *Sms2* deficiency on SMS activity, glucose tolerance, and insulin tolerance. Mice were fed a chow diet. (A) Tissue SMS activity measurements in *Sms2* KO and WT mice; (B) glucose tolerance test; (C) insulin tolerance test. Values are means ± SD (n = 10). *, $P < 0.01$.

to test whether it had a direct effect on insulin signaling. We found that after insulin treatment, exogenous ceramide (20 and 40 μM) increased Atk phosphorylation (Fig. 10F and H). These results indicate that exogenous SM and ceramide levels modulate insulin signaling in opposite directions.

DISCUSSION

While we were preparing and revising the manuscript, S. Mitsutake et al. reported that *Sms2* deficiency modifies SM levels in hepotocyte lipid rafts, resulting in obesity, fatty liver, and type 2 diabetes (38). However, those authors did not report the consequence of *Sptlc2* deficiency.

In this study, we have demonstrated that both heterozygous *Sptlc2*-deficient (*Sptlc2*$^{+/-}$) and *Sms2*-deficient mice have significantly more insulin sensitivity than WT animals. We attribute this primarily to the reduction of SM in plasma membrane SM-rich microdomains, and not to plasma membrane ceramide levels.

TABLE 4. Mouse tissue lipid analysis by LC-MS/MS (on chow)[a]

Tissue and lipid	WT	*Sms2* KO
Liver		
SM (nmol/mg)	1.92 ± 0.25	1.35 ± 0.11*
PC (nmol/mg)	29.37 ± 2.55	28.53 ± 3.12
Cer (ng/mg)	135.51 ± 19.20	188.62 ± 17.41*
S1P (ng/mg)	16.17 ± 0.57	15.15 ± 1.91
GlyCer (ng/mg)	161.03 ± 27.01	159.31 ± 13.73
Adipose		
SM (nmol/mg)	0.45 ± 0.03	0.31 ± 0.06*
PC (nmol/mg)	1.21 ± 0.19	1.28 ± 0.27
Cer (ng/mg)	9.11 ± 0.31	15.27 ± 0.33*
GlyCer (ng/mg)	1.01 ± 0.11	0.99 ± 0.12
Skeletal muscle		
SM (nmol/mg)	0.50 ± 0.03	0.39 ± 0.02*
PC (nmol/mg)	7.79 ± 0.55	8.33 ± 0.72
Cer (ng/mg)	33.41 ± 3.15	59.72 ± 6.92*
GlyCer (ng/mg)	66.38 ± 8.81	60.64 ± 9.50

[a] Values are means ± SD (n = 4). *, $P < 0.05$ compared to WT. Cer, ceramide; Glycer, glucosylceramide; S1P, sphingosine-1-phosphate.

A previous study indicated that treatment with myriocin, a potent SPT inhibitor, effectively ameliorates glucocorticoid-, saturated fat-, and obesity-induced insulin resistance (17). Those authors attributed the effect to the reduction of ceramide in tissues. However, SM levels in the tissues, especially in the cell plasma membranes, were not evaluated.

The role of cellular ceramide in insulin resistance is controversial. Ceramide is one of the main second messengers produced by *de novo* sphingolipid synthesis and sphingomyelinase-mediated hydrolysis of SM. There are two possibilities linking ceramide and insulin resistance. First, ceramide may block the translocation of Akt/PKB to plasma membranes (55). It has also been reported that ceramide inactivation of Akt/PKB requires the atypical protein kinase C (PKC) isoform PKCδ (45). Second, ceramide may impair the action of insulin by facilitating signaling pathways initiated by inflammatory cytokines, such as tumor necrosis factor alpha (which activates serine/threonine kinases, e.g., c-Jun N-terminal kinase or IKK) that are known to impair insulin signaling (18). However, it has also been reported that various glycosphingolipid synthase inhibitors augment insulin-stimulated phosphorylation of the insulin receptor, as well as Akt/PKB and/or mTOR phosphorylation, in the skeletal muscle (72) and liver (2, 72) of obese rodents, without altering ceramide levels. While ceramide accumulates in some insulin-resistant animal models (9, 54), it fails to do so in lipid-infused animals (24, 69). The relative increase of ceramide in obese rodents and humans is typically rather small (1, 58). Moreover, it is not known whether muscle ceramide con-

TABLE 5. Mouse plasma lipid and free fatty acid measurements (on chow)[a]

Mouse genotype	FFA (mM)	TG (mg/dl)	SM (mg/dl)	Chol (mg/dl)	PC (mg/dl)
WT	1.0 ± 0.3	63 ± 11	20 ± 5	86 ± 11	112 ± 13
*Sms2*KO	0.6 ± 0.2*	50 ± 5	13 ± 2*	92 ± 15	115 ± 25

[a] Values are means ± SD (n = 8). *, $P < 0.05$ compared to WT. FFA, free fatty acids; TG, triglycerol; Chol, cholesterol.

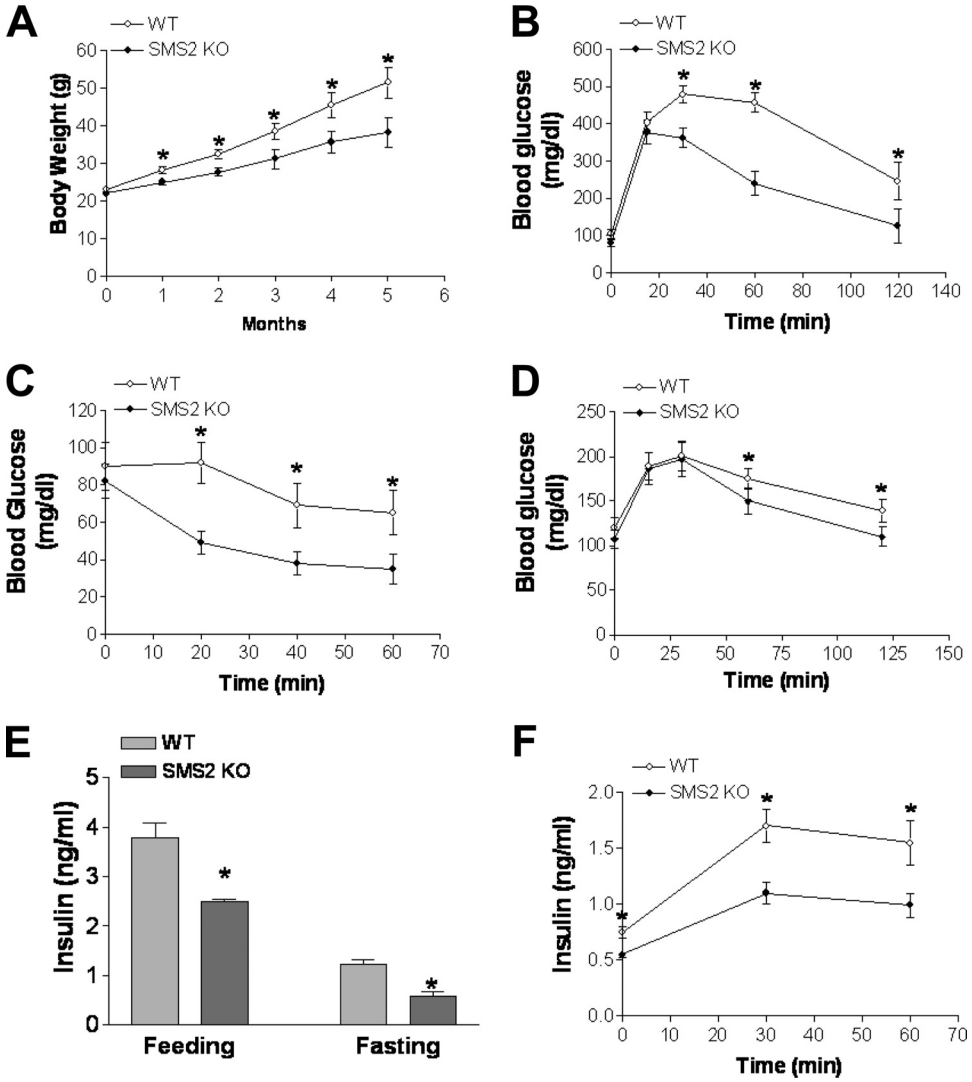

FIG. 9. Effects of *Sms2* deficiency on diet-induced body weight gain, glucose tolerance, insulin tolerance, pyruvate tolerance, and plasma insulin levels. (A) Quantitative display of body weight gain in *Sms2* KO and WT mice during the 20-week high-fat-diet feeding; (B) glucose tolerance test; (C) insulin tolerance test; (D) pyruvate tolerance test; (E) fasting and feeding plasma insulin level measurements; (F) plasma insulin levels after glucose injection. Values are means ± SD ($n = 10$). *, $P < 0.01$.

tent is a major factor in muscle insulin sensitivity. Adams et al. demonstrated that ceramide content is increased in skeletal muscles from obese, insulin-resistant humans (1), while Skovbro et al. found that human skeletal muscle ceramide content is not a major factor in muscle insulin sensitivity (52). It has been reported that GLUT4 translocation in 3T3-L1 adipocytes is a process mediated by a ceramide signaling route (63), but conflicting data from 3T3-L1 adipocytes and skeletal muscle suggest otherwise (29). Studies also seem to indicate that NF-κB activation can be triggered by increased ceramide levels (50). On the contrary, it has been shown that ceramide is not necessary for NF-κB activation, or it may even inhibit it (7). We and others have noticed that myriocin treatment not only reduces ceramide but also SM and glycosphingolipid levels (8, 16, 42).

Our findings suggest that cellular ceramide levels might not be the major mediator of insulin resistance. We found that *Sptlc2* heterozygous deficiency causes significant induction, rather than reduction, of ceramide levels in the liver of animals on both chow and high-fat, high-caloric diets (Table 2), while ceramide levels in liver plasma membranes are significantly decreased (Table 3). Also, we found no significant changes of ceramide levels in the adipose tissues or the muscles (Table 2) of animals on either diet. More importantly, we found that *Sms2* deficiency significantly increased ceramide levels in the liver, adipose tissues, and muscles (Table 4), while ceramide levels in liver plasma membranes were not significantly changed (Table 3). However, these animals demonstrate significantly increased insulin sensitivity, as shown by high-fat diet-induced body weight gain (Fig. 9A), glucose tolerance and insulin tolerance studies (Fig. 8B and C and 9B and C), and liver insulin-mediated Akt activation (Fig. 10C and D).

SM levels within cell plasma membranes, especially lipid rafts, are important in insulin signaling. The integrity of plasma

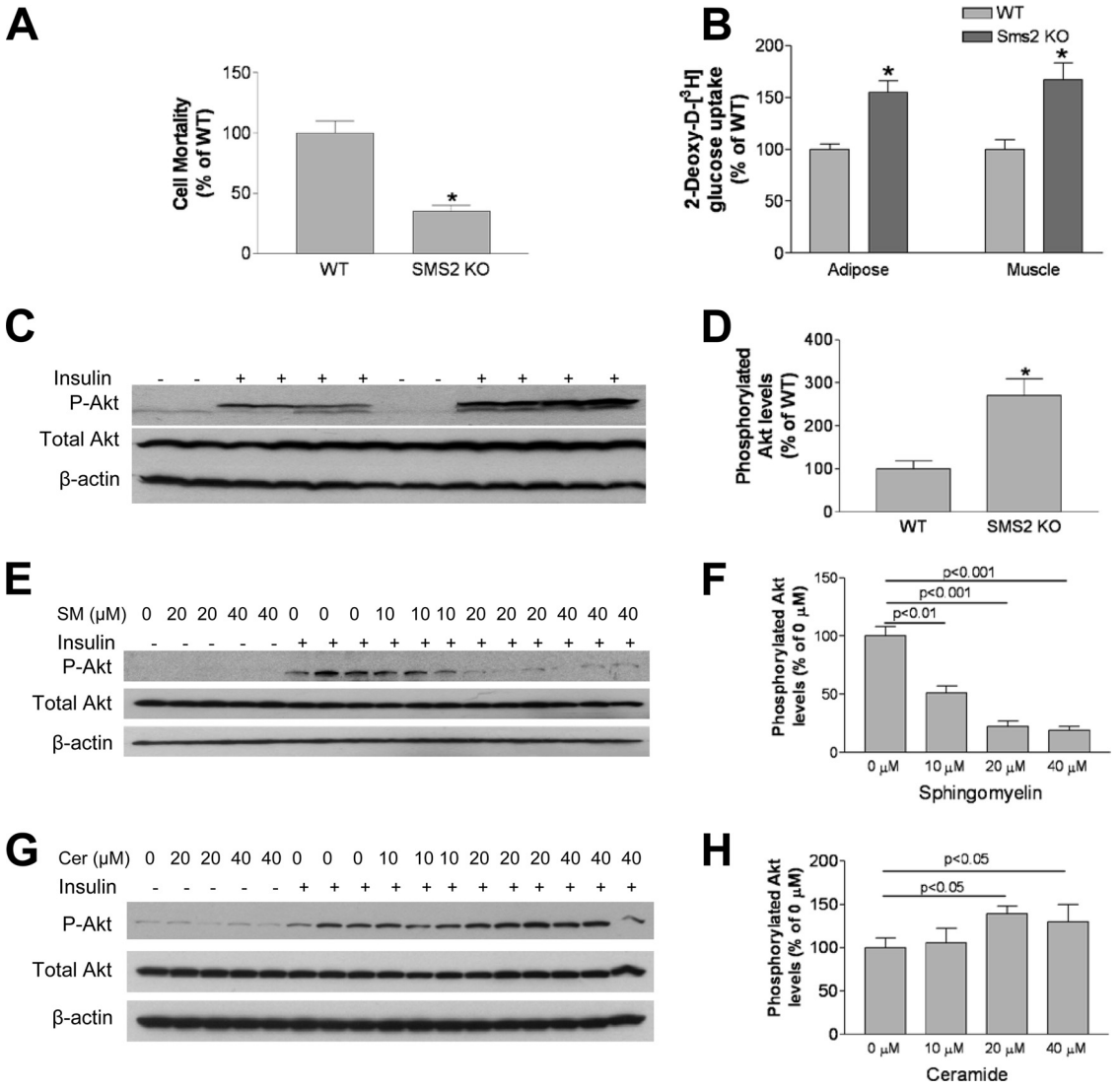

FIG. 10. Effects of *Sms2* deficiency on insulin signaling. (A) Lysenin-mediated cell lysis assay. (B) Liver Akt phosphorylation measurement. (C) Quantitative display of Akt phosphorylation. (D) Effects of exogenous SM on Akt phosphorylation. HepG2 cells were incubated with exogenous SM at 0, 10, 20, or 40 μM for 5 h; the cells were then treated with 100 nM insulin for 10 min, and Akt phosphorylation in whole-cell homogenates was measured. (E) Quantitative display of phosphorylated Akt. (F) Effects of exogenous ceramide ($C_{16:0}$) on Akt phosphorylation. HepG2 cells were incubated with 0, 10, 20, or 40 μM exogenous ceramide for 5 h; the cells were then treated with 100 nM insulin for 10 min, and Akt phosphorylation in whole-cell homogenates was measured. (G) Quantitative display of phosphorylated Akt. Values are means ± SD ($n = 5$). *, $P < 0.01$.

membranes is critical for insulin receptor autophosphorylation, and insulin resistance may be related to a plasma membrane lipid disorder (22). Membrane microdomains (lipid rafts) are now recognized as critical for proper compartmentalization of insulin signaling (21, 22), but their role in the pathogenesis of insulin resistance has not been completely investigated. Lipid rafts are highly enriched in cholesterol, glycosphingolipids, and SM (51). Manipulation of membrane cholesterol and glycosphingolipid has an important impact on insulin signaling (2, 22, 28, 43, 67, 72). Since SM is one of the major lipid components in lipid rafts, it is conceivable that diminished SM in plasma membranes could have an important impact on insulin signaling. Indeed, we found in this study that *Sptlc2*$^{+/-}$ mice have decreased hepatocyte plasma membrane SM levels, as evaluated by lysenin-mediated cell lysis (Fig. 7A) and SM direct measurement (Table 3). They also have increased tyrosine-phosphorylated insulin receptor in the lipid rafts (Fig. 7D and E), which increases insulin sensitivity. More importantly, we found that *Sms2* deficiency significantly decreases SM levels in the liver, adipose tissues, and muscles (Table 4) and in liver plasma membranes (Table 3). It significantly increases insulin sensitivity. These results indicate that *Sms2* deficiency appears to have phenotypes similar to *Sptlc2* partial deficiency, in terms of decreased SM levels in tissues and liver plasma membranes and increased insulin sensitivity.

Heterozygous *Sptlc2* deficiency and *Sms2* deficiency cause a significant decrease of plasma free fatty acid levels (Tables 1 and 5). It is well known that elevation of free fatty acid is

closely related to insulin resistance and metabolic syndrome (6, 48). This *Sptlc2* heterozygous deficiency- or *Sms2* deficiency-mediated free fatty acid effect may also contribute to an improvement of insulin sensitivity *in vivo*. This possibility deserves further investigation.

The *de novo* SM synthesis pathway also influences the formation of glycoceramides, among them GM3, which is a well-known mediator for insulin resistance (28). However, we found no significant changes of glucosylceramides or GM3 in *Sptlc2*$^{+/-}$ mouse plasma, tissues, or liver plasma membranes (Tables 2 and 3). This result is different from that after myriocin treatment, which can significantly decrease glucosylceramide levels (8). Moreover, *Sms2* deficiency does not influence glucosylceramides or GM3 in liver plasma membranes (Table 3). These results suggest that glycosphingolipids might not be responsible for the improvement of insulin sensitivity in our mutant mice.

The SM biosynthetic pathway also influences the formation of diacylglycerol (DAG) (37), a glycerolipid previously implicated in lipid-induced insulin resistance (69). However, high-fat, high-calorie-fed *Sptlc2*$^{+/-}$ mice did not have significantly reduced plasma or liver DAG levels compared with controls (Table 2), indicating that DAG might not be the regulator of insulin resistance in our models. This conclusion is consistent with the results of a recent study in which myriocin was used as the primary tool (17).

SPT activity is increased in *Apoe* KO mice (25), a well-known mouse model for atherosclerosis (44, 71). This increase contributes to the hypersphingomyelinemia in these animals (25). We and other researchers have found that myriocin treatment significantly reduces atherosclerosis in *Apoe* KO mice (8, 16, 42). We attribute this effect to the reduction of plasma SM levels, which are an independent risk factor for the disease (27, 49). However, the increased insulin sensitivity after myriocin treatment (17) might also contribute to the reduction of the disease, since insulin resistance and atherosclerosis are closely related.

Our conclusions are as follows: (i) both partial *Sptlc2* deficiency and *Sms2* deficiency enhance insulin sensitivity; (ii) both deficiencies decrease plasma membrane SM levels, which contribute to the enhancement of insulin sensitivity; (iii) *Sptlc2* deficiency decreases ceramide while *Sms2* deficiency increases it, and so ceramide is probably not the regulator of insulin sensitivity; (iv) there were no significant changes of glucosylceramide or GM3 levels in the tissues or plasma membrane, and so they might not be a regulator of insulin sensitivity under either deficient condition; and (v) SPT or SMS2 inhibition is a promising pharmacological approach for the treatment of insulin resistance and metabolic syndrome.

ACKNOWLEDGMENTS

This work was supported by a grant from the American Heart Association (grant-in-aid 0755922T to X.C.J.), National Institutes of Health grant HL-64735 to X.C.J., and a research award from Genzyme, Inc.

REFERENCES

1. **Adams, J. M., II, et al.** 2004. Ceramide content is increased in skeletal muscle from obese insulin-resistant humans. Diabetes **53:**25–31.
2. **Aerts, J. M., et al.** 2007. Pharmacological inhibition of glucosylceramide synthase enhances insulin sensitivity. Diabetes **56:**1341–1349.
3. **Chang, L., S. H. Chiang, and A. R. Saltiel.** 2004. Insulin signaling and the regulation of glucose transport. Mol. Med. **10:**65–71.
4. **de Mello, V. D., et al.** 2009. Link between plasma ceramides, inflammation and insulin resistance: association with serum IL-6 concentration in patients with coronary heart disease. Diabetologia **52:**2612–2615.
5. **Drab, M., et al.** 2001. Loss of caveolae, vascular dysfunction, and pulmonary defects in caveolin-1 gene-disrupted mice. Science **293:**2449–2452.
6. **Eckel, R. H., S. M. Grundy, and P. Z. Zimmet.** 2005. The metabolic syndrome. Lancet **365:**1415–1428.
7. **Gamard, C. J., G. S. Dbaibo, B. Liu, L. M. Obeid, and Y. A. Hannun.** 1997. Selective involvement of ceramide in cytokine-induced apoptosis. Ceramide inhibits phorbol ester activation of nuclear factor κB. J. Biol. Chem. **272:** 16474–16481.
8. **Glaros, E. N., et al.** 2007. Inhibition of atherosclerosis by the serine palmitoyl transferase inhibitor myriocin is associated with reduced plasma glycosphingolipid concentration. Biochem. Pharmacol. **73:**1340–1346.
9. **Gorska, M., A. Dobrzyn, M. Zendzian-Piotrowska, and J. Gorski.** 2004. Effect of streptozotocin-diabetes on the functioning of the sphingomyelin-signalling pathway in skeletal muscles of the rat. Horm. Metab. Res. **36:**14–21.
10. **Gustavsson, J., et al.** 1999. Localization of the insulin receptor in caveolae of adipocyte plasma membrane. FASEB J. **13:**1961–1971.
11. **Hailemariam, T. K., et al.** 2008. Sphingomyelin synthase 2 deficiency attenuates NFκB activation. Arterioscler. Thromb. Vasc. Biol. **28:**1519–1526.
12. **Han, G., et al.** 2009. Identification of small subunits of mammalian serine palmitoyltransferase that confer distinct acyl-CoA substrate specificities. Proc. Natl. Acad. Sci. U. S. A. **106:**8186–8191.
13. **Hanada, K., et al.** 1997. A mammalian homolog of the yeast LCB1 encodes a component of serine palmitoyltransferase, the enzyme catalyzing the first step in sphingolipid synthesis. J. Biol. Chem. **272:**32108–32114.
14. **Hojjati, M. R., and X. C. Jiang.** 2006. Rapid, specific, and sensitive measurements of plasma sphingomyelin and phosphatidylcholine. J. Lipid Res. **47:**673–676.
15. **Hojjati, M. R., Z. Li, and X. C. Jiang.** 2005. Serine palmitoyl-CoA transferase (SPT) deficiency and sphingolipid levels in mice. Biochim. Biophys. Acta **1737:**44–51.
16. **Hojjati, M. R., et al.** 2005. Effect of myriocin on plasma sphingolipid metabolism and atherosclerosis in apoE-deficient mice. J. Biol. Chem. **280:** 10284–10289.
17. **Holland, W. L., et al.** 2007. Inhibition of ceramide synthesis ameliorates glucocorticoid-, saturated-fat-, and obesity-induced insulin resistance. Cell. Metab. **5:**167–179.
18. **Holland, W. L., and S. A. Summers.** 2008. Sphingolipids, insulin resistance, and metabolic disease: new insights from in vivo manipulation of sphingolipid metabolism. Endocr. Rev. **29:**381–402.
19. **Hornemann, T., S. Richard, M. F. Rutti, Y. Wei, and A. von Eckardstein.** 2006. Cloning and initial characterization of a new subunit for mammalian serine-palmitoyltransferase. J. Biol. Chem. **281:**37275–37281.
20. **Huitema, K., J. van den Dikkenberg, J. F. Brouwers, and J. C. Holthuis.** 2004. Identification of a family of animal sphingomyelin synthases. EMBO J. **23:**33–44.
21. **Ikonen, E., and S. Vainio.** 2005. Lipid microdomains and insulin resistance: is there a connection? Sci. STKE 2005:pe3.
22. **Inokuchi, J.** 2006. Insulin resistance as a membrane microdomain disorder. Biol. Pharm. Bull. **29:**1532–1537.
23. **Ishitsuka, R., A. Yamaji-Hasegawa, A. Makino, Y. Hirabayashi, and T. Kobayashi.** 2004. A lipid-specific toxin reveals heterogeneity of sphingomyelin-containing membranes. Biophys. J. **86:**296–307.
24. **Itani, S. I., N. B. Ruderman, F. Schmieder, and G. Boden.** 2002. Lipid-induced insulin resistance in human muscle is associated with changes in diacylglycerol, protein kinase C, and IκB-α. Diabetes **51:**2005–2011.
25. **Jeong, T., et al.** 1998. Increased sphingomyelin content of plasma lipoproteins in apolipoprotein E knockout mice reflects combined production and catabolic defects and enhances reactivity with mammalian sphingomyelinase. J. Clin. Invest. **101:**905–912.
26. **Jiang, X. C., et al.** 2005. Phospholipid transfer protein deficiency impairs apolipoprotein-B secretion from hepatocytes by stimulating a proteolytic pathway through a relative deficiency of vitamin E and an increase in intracellular oxidants. J. Biol. Chem. **280:**18336–18340.
27. **Jiang, X. C., et al.** 2000. Plasma sphingomyelin level as a risk factor for coronary artery disease. Arterioscler. Thromb. Vasc. Biol. **20:**2614–2618.
28. **Kabayama, K., et al.** 2007. Dissociation of the insulin receptor and caveolin-1 complex by ganglioside GM3 in the state of insulin resistance. Proc. Natl. Acad. Sci. U. S. A. **104:**13678–13683.
29. **Kralik, S. F., P. Liu, B. J. Leffler, and J. S. Elmendorf.** 2002. Ceramide and glucosamine antagonism of alternate signaling pathways regulating insulin- and osmotic shock-induced glucose transporter 4 translocation. Endocrinology **143:**37–46.
30. **Landry, Y. D., et al.** 2006. ATP-binding cassette transporter A1 expression disrupts raft membrane microdomains through its ATPase-related functions. J. Biol. Chem. **281:**36091–36101.

31. **Langeveld, M., and J. M. Aerts.** 2009. Glycosphingolipids and insulin resistance. Prog. Lipid Res. **48:**196–205.
32. **Li, Z., et al.** 2007. Inhibition of sphingomyelin synthase (SMS) affects intracellular sphingomyelin accumulation and plasma membrane lipid organization. Biochim. Biophys. Acta **1771:**1186–1194.
33. **Liu, H., Y. Guz, M. H. Kedees, J. Winkler, and G. Teitelman.** 2010. Precursor cells in mouse islets generate new beta-cells in vivo during aging and after islet injury. Endocrinology **151:**520–528.
34. **Liu, J., et al.** 2009. Macrophage sphingomyelin synthase 2 deficiency decreases atherosclerosis in mice. Circ. Res. **105:**295–303.
35. **Liu, J., X. Jiang, L. Zhou, H. Wang, and X. Han.** 2009. Co-firing of oil sludge with coal-water slurry in an industrial internal circulating fluidized bed boiler. J. Hazard. Mater. **167:**817–823.
36. **Merrill, A. H., Jr.** 1983. Characterization of serine palmitoyltransferase activity in Chinese hamster ovary cells. Biochim. Biophys. Acta **754:**284–291.
37. **Merrill, A. H., Jr., and D. D. Jones.** 1990. An update of the enzymology and regulation of sphingomyelin metabolism. Biochim. Biophys. Acta **1044:**1–12.
38. **Mitsutake, S., et al.** 2011. Dynamic modification of sphingomyelin in lipid microdomains controls development of obesity, fatty liver, and type 2 diabetes. J. Biol. Chem. **286:**28544–28555.
39. **Miyaji, M., et al.** 2005. Role of membrane sphingomyelin and ceramide in platform formation for Fas-mediated apoptosis. J. Exp. Med. **202:**249–259.
40. **Muller, G., et al.** 2001. Redistribution of glycolipid raft domain components induces insulin-mimetic signaling in rat adipocytes. Mol. Cell. Biol. **21:**4553–4567.
41. **Nagao, K., et al.** 2007. Enhanced apoA-I-dependent cholesterol efflux by ABCA1 from sphingomyelin-deficient Chinese hamster ovary cells. J. Biol. Chem. **282:**14868–14874.
42. **Park, T. S., et al.** 2004. Inhibition of sphingomyelin synthesis reduces atherogenesis in apolipoprotein E-knockout mice. Circulation **110:**3465–3471.
43. **Parpal, S., M. Karlsson, H. Thorn, and P. Stralfors.** 2001. Cholesterol depletion disrupts caveolae and insulin receptor signaling for metabolic control via insulin receptor substrate-1, but not for mitogen-activated protein kinase control. J. Biol. Chem. **276:**9670–9678.
44. **Plump, A. S., et al.** 1992. Severe hypercholesterolemia and atherosclerosis in apolipoprotein E-deficient mice created by homologous recombination in ES cells. Cell **71:**343–353.
45. **Powell, D. J., E. Hajduch, G. Kular, and H. S. Hundal.** 2003. Ceramide disables 3-phosphoinositide binding to the pleckstrin homology domain of protein kinase B (PKB)/Akt by a PKCζ-dependent mechanism. Mol. Cell. Biol. **23:**7794–7808.
46. **Razani, B., et al.** 2001. Caveolin-1 null mice are viable but show evidence of hyperproliferative and vascular abnormalities. J. Biol. Chem. **276:**38121–38138.
47. **Saltiel, A. R., and C. R. Kahn.** 2001. Insulin signalling and the regulation of glucose and lipid metabolism. Nature **414:**799–806.
48. **Savage, D. B., K. F. Petersen, and G. I. Shulman.** 2007. Disordered lipid metabolism and the pathogenesis of insulin resistance. Physiol. Rev. **87:**507–520.
49. **Schlitt, A., et al.** 2006. Further evaluation of plasma sphingomyelin levels as a risk factor for coronary artery disease. Nutr. Metab. (Lond.) **3:**5.
50. **Schutze, S., et al.** 1992. TNF activates NF-kappa B by phosphatidylcholine-specific phospholipase C-induced "acidic" sphingomyelin breakdown. Cell **71:**765–776.
51. **Simons, K., and E. Ikonen.** 1997. Functional rafts in cell membranes. Nature **387:**569–572.
52. **Skovbro, M., et al.** 2008. Human skeletal muscle ceramide content is not a major factor in muscle insulin sensitivity. Diabetologia **51:**1253–1260.
53. **Steppan, C. M., et al.** 2001. The hormone resistin links obesity to diabetes. Nature **409:**307–312.
54. **Straczkowski, M., et al.** 2004. Relationship between insulin sensitivity and sphingomyelin signaling pathway in human skeletal muscle. Diabetes **53:**1215–1221.
55. **Stratford, S., D. B. DeWald, and S. A. Summers.** 2001. Ceramide dissociates 3′-phosphoinositide production from pleckstrin homology domain translocation. Biochem. J. **354:**359–368.
56. **Tabas, I., K. J. Williams, and J. Boren.** 2007. Subendothelial lipoprotein retention as the initiating process in atherosclerosis: update and therapeutic implications. Circulation **116:**1832–1844.
57. **Toyoshima, Y., et al.** 2005. Leptin improves insulin resistance and hyperglycemia in a mouse model of type 2 diabetes. Endocrinology **146:**4024–4035.
58. **Turinsky, J., D. M. O'Sullivan, and B. P. Bayly.** 1990. 1,2-Diacylglycerol and ceramide levels in insulin-resistant tissues of the rat in vivo. J. Biol. Chem. **265:**16880–16885.
59. **Vacaru, A. M., et al.** 2009. Sphingomyelin synthase-related protein SMSr controls ceramide homeostasis in the ER. J. Cell Biol. **185:**1013–1027.
60. **Van der Luit, A. H., et al.** 2007. Resistance to alkyl-lysophospholipid-induced apoptosis due to downregulated sphingomyelin synthase 1 expression with consequent sphingomyelin- and cholesterol-deficiency in lipid rafts. Biochem. J. **401:**541–549.
61. **Virkamaki, A., K. Ueki, and C. R. Kahn.** 1999. Protein-protein interaction in insulin signaling and the molecular mechanisms of insulin resistance. J. Clin. Invest. **103:**931–943.
62. **Vuguin, P. M., et al.** 2006. Ablation of the glucagon receptor gene increases fetal lethality and produces alterations in islet development and maturation. Endocrinology **147:**3995–4006.
63. **Wang, C. N., L. O'Brien, and D. N. Brindley.** 1998. Effects of cell-permeable ceramides and tumor necrosis factor-alpha on insulin signaling and glucose uptake in 3T3-L1 adipocytes. Diabetes **47:**24–31.
64. **Weiss, B., and W. Stoffel.** 1997. Human and murine serine-palmitoyl-CoA transferase: cloning, expression and characterization of the key enzyme in sphingolipid synthesis. Eur. J. Biochem. **249:**239–247.
65. **Weyer, C., et al.** 2001. Hypoadiponectinemia in obesity and type 2 diabetes: close association with insulin resistance and hyperinsulinemia. J. Clin. Endocrinol. Metab. **86:**1930–1935.
66. **Yamaoka, S., M. Miyaji, T. Kitano, H. Umehara, and T. Okazaki.** 2004. Expression cloning of a human cDNA restoring sphingomyelin synthesis and cell growth in sphingomyelin synthase-defective lymphoid cells. J. Biol. Chem. **279:**18688–18693.
67. **Yamashita, T., et al.** 2003. Enhanced insulin sensitivity in mice lacking ganglioside GM3. Proc. Natl. Acad. Sci. U. S. A. **100:**3445–3449.
68. **Yang, X. L., Z. H. Xie, X. J. Jiang, Y. B. Huang, and J. K. Liu.** 2009. A new acridone alkaloid from Micromelum integerrimum. Chem. Pharm. Bull. (Tokyo) **57:**734–735.
69. **Yu, C., et al.** 2002. Mechanism by which fatty acids inhibit insulin activation of insulin receptor substrate-1 (IRS-1)-associated phosphatidylinositol 3-kinase activity in muscle. J. Biol. Chem. **277:**50230–50236.
70. **Yvan-Charvet, L., et al.** 2005. Deletion of the angiotensin type 2 receptor (AT2R) reduces adipose cell size and protects from diet-induced obesity and insulin resistance. Diabetes **54:**991–999.
71. **Zhang, S. H., R. L. Reddick, J. A. Piedrahita, and N. Maeda.** 1992. Spontaneous hypercholesterolemia and arterial lesions in mice lacking apolipoprotein E. Science **258:**468–471.
72. **Zhao, H., et al.** 2007. Inhibiting glycosphingolipid synthesis improves glycemic control and insulin sensitivity in animal models of type 2 diabetes. Diabetes **56:**1210–1218.